

- by standard phosphoramidite synthesis starting from C7-amino-link 500 Å CPG (Glen Research) and selective deprotection of the R-N(H)-Fmoc by treatment with 20% piperidine in DMF (v/v) at ambient temperature for 30 min. The 5'-alkylamino DNA was prepared from dT 2,000 Å CPG (Glen Research), followed by standard phosphoramidite synthesis and functionalization with a nonamethylene amino-alkyl linker [L. Wachter, J. A. Jablonski, K. L. Ramachandran, *Nucleic Acids Res.* **14**, 7985 (1986)]. Activation of racemic metal complex, coupling to DNA, and HPLC purification of the diastereomeric Δ-Rh and Λ-Rh conjugates was identical for 3'- and 5'-functionalized oligonucleotides [see (14)].
16. After 6 hours of irradiation at 400 nm, 5% repair of the thymine dimer was found in control samples lacking rhodium (light control) and represents the background repair by light in our experiments.
  17. To account for the repair efficiency observed in Rh-modified duplexes based on an intermolecular reaction, the duplex dimerization constant would be  $\sim 10^4 \text{ M}^{-1}$ . On the basis of the observed concentration dependence in repair and the comparison with the limiting results with noncovalently bound rhodium, we estimate the duplex dimerization constant instead to be  $\leq 10^3 \text{ M}^{-1}$ .
  18. Photocleavage reactions at 313 nm, measured by photoimaging, sensitively detect strand cleavage at several orders of magnitude lower intensity than required to detect rhodium reaction near the tethered end of the duplex in Rh-modified oligomers. Photocleavage reactions as a function of concentration of Rh-modified duplexes also indicate that interduplex reaction is negligible at duplex concentrations of  $\leq 25 \mu\text{M}$ .
  19. Assuming a 3.4 Å centroid-to-centroid distance between stacked base pairs, the separation between the intercalated phi ligand of the rhodium complex and the center of the thymine dimer is 19 Å for both the 5'-Rh- and 3'-Rh-tethered assemblies when the complex is intercalated between the third and fourth base pair from the end of the duplex. On the basis of the photocleavage pattern (Fig. 2), the closest distance between intercalator and thymine dimer along the helical axis appears to be 16 Å for both assemblies with intercalation in the fourth base step.
  20. For both diastereomers, direct photocleavage experiments (313 nm) show the metal complex to be fully bound by intercalation at these concentrations.
  21. J. K. Barton, *Science* **233**, 727 (1986).
  22. Nuclear magnetic resonance studies have suggested somewhat greater perturbations of the thymine dimer to its 3' side [J. Kemmink *et al.*, *Nucleic Acids Res.* **15**, 4645 (1987); J.-S. Taylor, D. S. Garrett, I. R. Brockie, D. L. Svoboda, J. Telsner, *Biochemistry* **29**, 8858 (1990)].
  23. To evaluate the stacking interaction of tethered rhodium into the DNA duplex, we measured the steady-state luminescence quenching of a stoichiometric amount of *rac*-Ru(phen)<sub>2</sub>dppz<sup>2+</sup> (phen, 1,10-phenanthroline; dppz, dipyrido[3,2-a:2',3'-c]phenazine) noncovalently bound to the duplex by intercalation of the dppz ligand for the individual assemblies. The amount of quenching provides a measure of the efficiency of electron transfer from electronically excited ruthenium to ground-state rhodium through the DNA helix and can be assumed, within an individual DNA sequence, to reflect the ability of rhodium to intercalate into the duplex (12). For the 3'-Rh-tethered 16-bp duplex (Table 1, top), luminescence quenching was 49% and 39% for Δ-Rh and Λ-Rh, respectively, versus luminescence of *rac*-Ru(phen)<sub>2</sub>dppz<sup>2+</sup> intercalated into the unmodified duplex (without thymine dimer). For the corresponding 5'-tethered rhodium duplex, luminescence quenching was 58% and 52% for Δ-Rh and Λ-Rh, respectively. The higher repair yields therefore correlate with higher quenching of ruthenium luminescence.
  24. An analogous sensitivity in long-range oxidation of guanine doublets to intervening bulges in DNA has been observed in our laboratory (D. Hall and J. K. Barton, unpublished results).
  25. M. A. Rosen, L. Shapiro, D. J. Patel, *Biochemistry* **31**, 4015 (1992); M. W. Kalnik, D. G. Norman, B. F. Li, P. F. Swann, D. J. Patel, *J. Biol. Chem.* **265**, 636 (1990).
  26. Direct photocleavage studies with Rh(phi)<sub>2</sub>DMB<sup>3+</sup> on the duplex containing a thymine dimer do not suggest preferential binding of the rhodium adjacent to the dimer.
  27. The  $T_m$  for unmodified dimer-containing duplexes increased by 2°C in the presence of 1 equivalent of Rh(phi)<sub>2</sub>DMB<sup>3+</sup> and by 5°C with Δ-Rh tethered to the 5'-terminus.
  28. D. G. Vassilyev *et al.*, *Cell* **83**, 773 (1995).
  29. Supported by NIH grant GM49216, a postdoctoral fellowship from the Cancer Research Fund of the Damon Runyon-Walter Winchell Foundation (P.J.D.), and an NSF predoctoral fellowship (R.E.H.). We thank N. J. Turro and E. D. A. Stemp for helpful discussions.
- 24 July 1996; accepted 23 January 1997

## Requirement of the DEAD-Box Protein Ded1p for Messenger RNA Translation

Ray-Yuan Chuang, Paul L. Weaver, Zheng Liu, Tien-Hsien Chang\*

The *DED1* gene, which encodes a putative RNA helicase, has been implicated in nuclear pre-messenger RNA splicing in the yeast *Saccharomyces cerevisiae*. It is shown here by genetic and biochemical analysis that translation, rather than splicing, is severely impaired in two newly isolated *ded1* conditional mutants. Preliminary evidence suggests that the protein Ded1p may be required for the initiation step of translation, as is the distinct DEAD-box protein, eukaryotic initiation factor 4A (eIF4A). The *DED1* gene could be functionally replaced by a mouse homolog, *PL10*, which suggests that the function of Ded1p in translation is evolutionarily conserved.

Eukaryotic translation initiation requires many factors to promote the binding of the 80S ribosome to the initiation codon in the mRNA (1, 2). Binding of the 43S preinitiation complex, which is derived from the 40S subunit of the 80S ribosome, to mRNA is a rate-limiting step that requires three eukaryotic initiation factors: 4A (eIF4A), 4B, and 4F (consisting of three subunits, eIF4A, eIF4E, and eIF4G). It has been proposed (3) that eIF4B and eIF4F together form an RNA-helicase complex that binds to the 5' cap of the mRNA through eIF4E. This complex then unwinds duplex structures in the 5' untranslated region, thereby permitting the 43S complex to scan the mRNA until the first AUG codon is selected. eIF4A is thought to play a major role in this unwinding process, because it can unwind short RNA duplexes in vitro in conjunction with eIF4B (4). eIF4A belongs to the evolutionarily conserved DEAD-box protein family (5), whose members share nine highly conserved amino acid regions, including the distinct Asp-Glu-Ala-Asp (DEAD) sequence. Here, we report that translation in yeast requires another DEAD-box protein, Ded1p, whose function appears to be conserved in evolution.

The *DED1* gene was originally identified as an essential open reading frame adjacent to *HIS3* (6). Ded1p was hypothesized to function in nuclear pre-mRNA splicing because *spp81-1*, a mutant allele of *DED1*, suppresses the growth and splicing defects caused by the *prp8-1* mutation (7). More recently, it was reported that overexpression of *DED1* can suppress the growth defect of an RNA polymerase III (Pol III) mutant, which suggests that Ded1p can also influence Pol III transcription, although it may not normally participate in this process (8). To investigate the function of Ded1p, we isolated two *ded1* cold-sensitive mutants (9). The *ded1-120* and *ded1-199* alleles yield mutant forms of Ded1p with predicted amino acid substitutions of Gly<sup>108</sup> → Asp and Gly<sup>494</sup> → Asp (*ded1-120*) and Gly<sup>368</sup> → Asp (*ded1-199*). At 25°C both mutants grew substantially slower than did the wild-type strain, and at 15°C they did not grow.

We first examined the *ded1-120* and *ded1-199* mutants for splicing defects by Northern (RNA) blotting. No splicing defects were detected in either *ded1* mutant after shifting cultures to 15°C for 2 hours. This observation was in sharp contrast to the aberrant rise in *ACT1* pre-mRNA levels and decline in mature *CRY1* mRNA levels in control strains *prp2* and *prp11*, which harbor splicing mutations (10).

Instead, we found that, at 15°C, the incorporation of [<sup>35</sup>S]methionine into acid-precipitable peptides in each *ded1* mutant strain was ~10% of that incorporated in the isogenic wild-type strain. This inhibition of protein synthesis seemed to be gen-

R.-Y. Chuang, Molecular, Cellular, and Developmental Biology Program, Ohio State University, Columbus, OH 43210, USA.

P. L. Weaver and Z. Liu, Department of Molecular Genetics, Ohio State University, Columbus, OH 43210, USA.  
T.-H. Chang, Department of Molecular Genetics and Molecular, Cellular, and Developmental Biology Program, Ohio State University, Columbus, OH 43210, USA.

\*To whom correspondence should be addressed. E-mail: chang.108@osu.edu

eral, because the production of most, if not all, of the polypeptides appeared to be equally reduced in the *ded1* mutants (Fig. 1A). When the *ded1-199* mutant strain was shifted to 15°C for 2 hours, there was a marked increase in the level of 80S ribosomes and a decline in the level of polyribosomes (Fig. 1, B and C). The changes in the polyribosome profile were readily detected 5 min after temperature shift (Fig. 1D), which suggested that Ded1p likely plays a direct role in translation initiation. Fractionation of the *ded1* mutant extracts in high-salt sucrose gradients resulted in a complete dissociation of the 80S ribosomes into 40S and 60S subunits, indicating that the accumulated 80S ribosomes were either pre-initiation complexes or 80S couples (10, 11). These phenotypes were not the result of mRNA export defects, because in situ mRNA localization assays (12) revealed no nuclear accumulation of polyadenylated [poly(A)<sup>+</sup>] RNAs in *ded1* mutants after temperature shift for up to 22 hours. Nor were these phenotypes caused by rapid degradation of the poly(A)<sup>+</sup> RNAs, because the steady-state levels of transcripts from *ACT1*, *CYH2*, *CUP1*, and *CRY1* genes in *ded1* mutants were similar to those of the wild-type cells 4 hours after temperature shift (10).

To test whether Ded1p is present in the cytoplasm, we constructed a yeast strain in which the wild-type *DED1* gene was replaced with a *DED1*-Protein A gene fusion. The fusion protein was functional in vivo, because the growth rate and the polyribosome profile of its host strain (*DED1-PA*) were nearly indistinguishable from those of the wild-type strain. A Ded1p-Protein A fusion protein (Ded1p-PA) of the predicted size (92 kD) was detected by normal rabbit serum in extracts prepared from the *DED1-PA* strains, but not from the wild-type strain (Fig. 2A). Indirect immunofluorescence microscopy revealed that Ded1p-PA staining was restricted to the cytoplasm (Fig. 2, C and D). Control experiments with strains expressing only the wild-type Ded1p yielded no fluorescence signal, and an identical cytoplasmic staining pattern was observed in a strain expressing a hemagglutinin-tagged Ded1p (10). Although we cannot rule out the possibility that a minor fraction of Ded1p is present in the nucleus or that Ded1p shuttles between the cytoplasm and the nucleus, our results strongly suggest that Ded1p is predominantly cytoplasmic, consistent with its proposed role in translation.

Independent mutations in the same biochemical pathway may act synergistically to yield a lethal phenotype (13). We tested the possibility that the *ded1-120* and *ded1-199* mutations are synthetically lethal to a temperature-sensitive mutation in *TIF1* (14), which encodes yeast eIF4A (15).

Strains harboring the double mutations *ded1 tif1*, *ded1 prp28*, *ded1 prt1*, and *ded1 sis1* were constructed and examined under growth conditions permissive to all the single mutants. Prp28p is a member of the DEAD-box protein family involved in pre-mRNA splicing (16), Prt1p is an eIF3 subunit (17), and Sis1p is thought to mediate the dissociation of protein complexes in the

translation machinery (11). Lethality resulted only when the *ded1-120* (10) or *ded1-199* mutations were combined with the *tif1* mutation (Fig. 3). Thus, the synthetic lethality was gene-specific and was not simply dependent on the presence of two mutant DEAD-box protein genes. Because *DED1* and *TIF1* are both essential genes and the observed synthetic lethality is not allelic-

**Fig. 1.** Defective protein synthesis in *ded1-120* and *ded1-199* mutants. **(A)** Protein synthesis as measured by [<sup>35</sup>S]methionine incorporation. Lanes 1 and 4, wild-type strain; lanes 2 and 5, *ded1-120* strain; lanes 3 and 6, *ded1-199* strain. Three OD<sub>600</sub> units of cells were resuspended in 1 ml of YPD (1% yeast extract, 2% peptone, and 2% dextrose) and incubated at 30° or 15°C. After 5 min, 20 μCi of L-[<sup>35</sup>S]methionine (>1000 Ci/mmol, DuPont-NEN) was added and the cells were again incubated at 30° or 15°C for 1 hour. The collected cells were broken by vortexing with glass beads. Proteins in the supernatant were analyzed by electrophoresis on an 8% SDS polyacrylamide gel and autoradiography. **(B)** and **(C)** Polyribosome profiles of the wild-type **(B)** or *ded1-199* **(C)** strains after temperature shift to 15°C for 2 hours. **(D)** Similar to **(C)**, except that the cultures were shifted to 15°C for 0, 5, 10, and 15 min. Cells were grown initially to 0.5 to 0.8 OD<sub>600</sub> unit at 30°C and shifted to 15°C for the time indicated. Polyribosomes were analyzed on sucrose density gradients (7 to 47%) as in (26).

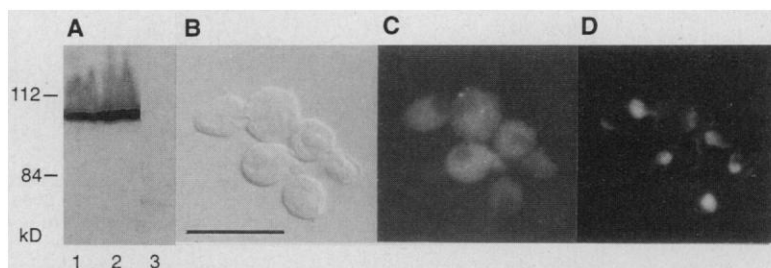
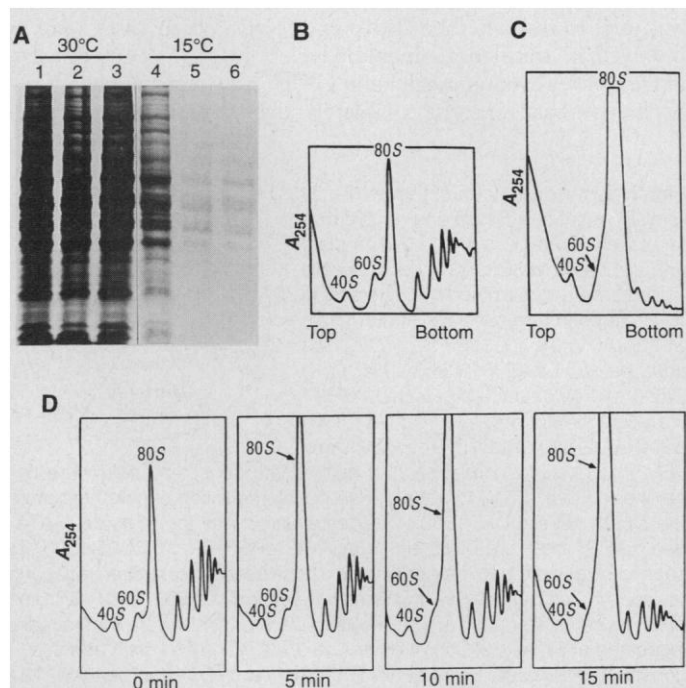


**Fig. 2.** Cytoplasmic localization of Ded1p-PA. **(A)** Immunoblot analysis of crude extracts from the *DED1-PA* strain (lanes 1 and 2, two independent isolates) or from the wild-type strain (lane 3). Immunoblots were developed with normal rabbit serum at 1:2500 dilution and Protein G-horseradish peroxidase conjugate (Bio-Rad) at 1:6000 dilution, followed by chemiluminescence detection (ECL system, Amersham) of Ded1p-PA. The *DED1-PA* recombinant clone was constructed by fusing in frame a 651-bp polymerase chain reaction product containing the IgG-binding domain of Protein A to the *Aat* II site immediately upstream of the stop codon of the wild-type *DED1* gene carried on pRS315. The *Aat* II site was engineered by site-specific mutagenesis using an oligonucleotide primer (5'-TGCTGAAATCAGACGTCACCAAGGAAGA-3'). This *DED1-PA* plasmid was introduced into a diploid strain [*MATa/α ded1::TRP1/ded1::TRP1 ura3-52/ura3-52 lys2-801/lys2-801 ade2-101/ade2-101 trp1-Δ1/trp1-Δ1 his3-Δ200/his3-Δ200 leu2-Δ1/leu2-Δ1* pDED1008 (*DED1/CEN/URA3*)]. After 5-FOA counterselection (9) of pDED1008, the resulting diploid strain was used for immunoblot analysis and indirect immunofluorescence microscopy (27). **(B)** to **(D)** Indirect immunofluorescence microscopy of *DED1-PA* cells. Cells viewed by Normarski optics **(B)**, cells stained first with purified normal rabbit IgG and then with Texas Red-conjugated goat antibody to rabbit IgG **(C)**, and cells stained by DAPI **(D)** are shown. Scale bar, 10 μm.

specific, the simplest interpretation for these data is that Tif1p and Ded1p play two independent but nonetheless related roles in translation. The inability to suppress the growth defects of *ded1* mutants by overexpression of *TIF1* (10) is consistent with this proposal. Our genetic analysis is further supported by the finding that a *ded1* mutation is also synthetically lethal to *cdc33-1*, which encodes a mutant eIF4E (18).

A yeast in vitro translation system (19) was used to test whether Ded1p is directly involved in translation. Immunodepletion of Ded1p-PA by immunoglobulin G (IgG)-Sepharose beads nearly completely abol-

ished translation activity as measured by a luciferase assay (Fig. 4A). This effect was apparently caused by the depletion of >90% of Ded1p-PA in the extract as judged by immunoblot analysis (10). Identical treatments of the wild-type extracts reduced the translation activity by only 40%, presumably as a result of nonspecific interactions of IgG-Sepharose beads with cellular components. Because the chemical half-lives of the luciferase transcripts in both cases were nearly identical (10), the loss of the translation activity was unlikely to have been a result of the rapid degradation of transcript upon Ded1p-PA deple-

tion. Addition of normal rabbit IgG to the Ded1p-PA extracts yielded a dose-dependent reduction of the translation activity but had no inhibitory effect on the wild-type extracts (Fig. 4B). To rule out nonspecific depletion, we used a glutathione-S-transferase (GST)-Ded1p fusion protein purified from *Escherichia coli* to reconstitute the translation activity. GST-Ded1p enhanced the translation activity in a dose-dependent manner to more than eight times that of the depleted extracts, whereas purified GST had no stimulatory effect on the translation activity (Fig. 4C).

Ded1p shares 53% amino acid sequence identity with the predicted gene product of a mouse transcript, *PL10*, which is thought to be involved in spermatogenesis (20). We thus tested whether *PL10* and *DED1* are functional homologs. When driven by the yeast glyceraldehyde-3-phosphate dehydrogenase promoter ( $P_{GPD}$ ) and carried on a yeast centromere plasmid, the *PL10* cDNA rescued the lethality of cells with a chromosomal *ded1* deletion (10). This functional complementation was specific, because a  $P_{GPD}$ -*PRP28* construct capable of complementing a lethal deletion of the *PRP28* gene failed to do so in the *ded1*-deletion background (10). This observation suggests that *PL10* may play a role in translation in the mouse.

It is unlikely that Ded1p plays a direct role in pre-mRNA splicing (Fig. 2C) (10) and Pol III transcription (8). We suggest that Ded1p may influence the production of factors involved in these two nuclear events, thereby mediating the genetic suppression indirectly. Although several novel factors, including a helicase-like protein, have been implicated in translation (21), subsequent biochemical analysis suggested otherwise (22). Our data thus provide evidence that at least two distinct DEAD-box proteins are indispensable for translation; such a situation is reminiscent of pre-mRNA splicing (23) and ribosomal biogenesis (24), in which multiple DEAD-box proteins are required. Although it is clear that eIF4A and Ded1p are functionally distinct, it remains possible that their functions partially overlap. Our results also raise the possibility that the involvement of *PL10* during the meiotic and haploid stages of mouse spermatogenesis is mediated by its function in translation. Because multiple *PL10*- and *DED1*-like genes are expressed in different mouse tissues (25), these genes are functionally important and have potential roles in regulating gene expression by means of differential translation.

**Fig. 3.** Synthetic lethality of the *ded1-199* and *tif1* mutations. Single and double mutants were streaked out on a 5-FOA plate and incubated at 30°C for 4 days. Double mutants were constructed by first crossing a *tif1* temperature-sensitive strain (strain SS13-3A; MAT $\alpha$  *tif1::HIS3* *tif2::ADE2* *his3* *ade2* *leu2* *trp1* *ura3* YCpLac33-*tif1*<sup>ts</sup>) to a *DED1* wild-type strain [MAT $\alpha$  *ded1::TRP1* *ura3-52* *lys2-801* *ade2-101* *trp1- $\Delta$ 1* *his3- $\Delta$ 200* *leu2- $\Delta$ 1* pDED1009 (*DED1/CEN/LEU2*)] to obtain a combination of appropriate genetic markers. The *tif1*<sup>ts</sup> allele on YCpLac33 was transferred to pRS317 to allow 5-FOA counterselection of cells harboring a *URA3* plasmid containing the *DED1* gene (pDED1008). The tester strains at the end are MAT $\alpha$  (or  $\alpha$ ) *tif1::HIS3* *tif2::ADE2* *ded1::TRP1* *his3* *ade2* *leu2* *trp1* *ura3* *lys2* pRS317-*tif1*<sup>ts</sup> pDED1008. To rule out synthetic lethality caused by genetic background variations, we used at least three independent tester strain isolates. To test for synthetic lethality, we individually transformed *DED1*, *ded1-120*, and *ded1-199* alleles carried on pRS315 into tester strains. The resulting transformants were then streaked out on 5-FOA plates and incubated at 27° or 30°C for 4 days. The *ded1 prt1*, *ded1 sis1*, and *ded1 prp28* double mutants were constructed similarly, using strain F294 (MAT $\alpha$  *prt1-1* *ade1* *leu2-3,112* *ura3-52*), strain CY732 (11) [MAT $\alpha$  *sis1::HIS3* *ade2-1* *trp1-1* *leu2-3,112* *his3-11,15* *ssd1-d2* *can1-100* (*sis1-85* on a *CEN/LEU2* plasmid)], and strain YTC95 (28) [MAT $\alpha$  *prp28::HIS3* *ura3-52* *lys2-801* *ade2-101* *trp1- $\Delta$ 1* *his3- $\Delta$ 200* *leu2- $\Delta$ 1* (*prp28-117* on a *CEN/LEU2* plasmid)]. The *prp28-117* mutant does not grow at 15°C.

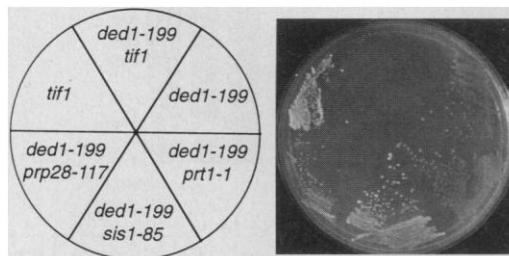
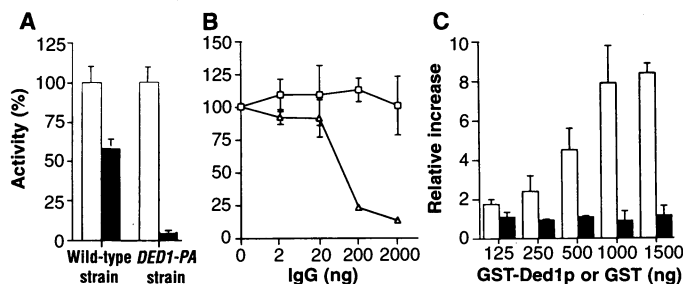


**Fig. 4.** Loss and restoration of Ded1p-dependent translation activity. (A) Immunodepletion of Ded1p-PA results in loss of translation activity. Data are expressed as the percent of luciferase produced in extracts treated with IgG-Sepharose (solid bars) and without treatment (open bars; 100% activity). Yeast extract (25  $\mu$ l) was mixed with IgG-Sepharose [10  $\mu$ l (bed volume), Pharmacia] and incubated at 4°C for 30 min. After centrifugation, 10  $\mu$ l of supernatant was used to assemble a 25- $\mu$ l translation reaction in the presence of 100 ng of capped-luciferase transcript with poly(A) tail (19). Reactions were incubated at 20°C for 1 hour. Luciferase was quantitated by luminescence emission using a luciferase assay (Promega). Experiments were repeated at least three times. (B) Neutralization of Ded1p-PA results in loss of translation activity. Data are expressed as the percent of luciferase produced in the absence of normal rabbit IgG in the wild-type ( $\square$ ) and *DED1-PA* ( $\Delta$ ) extracts. After 10  $\mu$ l of yeast extract was preincubated with increasing amounts of normal rabbit IgG at 4°C for 30 min, translation was assayed as in (A). (C) Restoration of Ded1p-dependent translation activity by addition of GST-Ded1p. Data are expressed as activity increase relative to the translation activity of depleted extract upon addition of GST-Ded1p (open bars) or GST (solid bars). The *DED1* coding region was fused in frame to the GST coding region on pGEX-2T (Pharmacia) and overexpressed in *E. coli* strain XL1-Blue (Stratagene). Affinity purification of GST-Ded1p and GST by glutathione agarose (Sigma) was done according to manufacturer's instructions (Pharmacia). After 10  $\mu$ l of the depleted extract was preincubated with increasing amounts of purified GST-Ded1p or GST for 15 min at 20°C, translation was assayed as in (A).



## REFERENCES AND NOTES

1. J. W. B. Hershey, *Annu. Rev. Biochem.* **60**, 717 (1991); W. C. Merrick, *Microbiol. Rev.* **56**, 291 (1992).

2. W. C. Merrick and J. W. B. Hershey, in *Translational Control*, J. W. B. Hershey, M. B. Mathews, N. Sonenberg, Eds. (Cold Spring Harbor Laboratory Press, Cold Spring Harbor, NY, 1996), pp. 31–69.
3. A. Pause and N. Sonenberg, *Curr. Opin. Struct. Biol.* **3**, 953 (1993).
4. F. Rozen *et al.*, *Mol. Cell. Biol.* **10**, 1134 (1990).
5. F. V. Fuller-Pace, *Trends Cell Biol.* **4**, 271 (1994).
6. K. Struhl and R. W. Davis, *J. Mol. Biol.* **136**, 309 (1980); K. Struhl, *Nucleic Acids Res.* **13**, 8587 (1985).
7. D. J. Jamieson, B. Rahe, J. Pringle, J. D. Beggs, *Nature* **349**, 715 (1991).
8. V. Thuillier, S. Stettler, A. Sentenac, P. Thuriaux, M. Werner, *EMBO J.* **14**, 351 (1995).
9. A 2.9-kb Xho I-Sal I DNA fragment containing the complete *DED1* gene (6) was subcloned into pRS315 (*CEN/LEU2*) to yield pDED1009 and incubated with hydroxylamine [R. S. Sikorski and J. D. Boeke, *Methods Enzymol.* **194**, 302 (1991)]. The mutagenized DNA was amplified and transformed into yeast strain YTC75 [*MATa ded1::TRP1 ura3-52 lys2-801 ade2-101 trp1-Δ1 his3-Δ200 leu2-Δ1* pDED1008 (*DED1/CEN/URA3*)]. Transformants on leucine-dropout plates were replica-plated onto 5-fluoroorotic acid (5-FOA) plates to identify conditional mutants that failed to grow at either 37° or 15°C. Linkage between the growth phenotype and the mutated *ded1* allele was verified by recloning the *ded1* insert and repeating the plasmid shuffling. Mutations in the *ded1* alleles were identified by DNA sequencing.
10. R.-Y. Chuang and T.-H. Chang, data not shown.
11. T. Zhong and K. T. Arndt, *Cell* **73**, 1175 (1993).
12. T. Kadowaki *et al.*, *J. Cell Biol.* **126**, 649 (1994).
13. L. Guarente, *Trends Genet.* **9**, 362 (1993).
14. S. R. Schmid and P. Linder, *Mol. Cell. Biol.* **11**, 3463 (1991).
15. P. Linder and P. P. Slonimski, *Proc. Natl. Acad. Sci. U.S.A.* **86**, 2286 (1989).
16. E. J. Strauss and C. Guthrie, *Genes Dev.* **5**, 629 (1991).
17. T. Naranda, S. E. MacMillan, J. W. B. Hershey, *J. Biol. Chem.* **269**, 32286 (1994).
18. J. de la Cruz and P. Linder, personal communication.
19. I. Hussain and M. J. Leibowitz, *Gene* **46**, 13 (1986); N. Iizuka, L. Najita, A. Franzusoff, P. Sarnow, *Mol. Cell. Biol.* **14**, 7322 (1994).
20. P. Leroy, P. Alzari, D. Sassoon, D. Wolgemuth, M. Fellous, *Cell* **57**, 549 (1989).
21. K. D. Gulyas and T. F. Donahue, *ibid.* **69**, 1031 (1992); H. Yoon, S. Miller, E. K. Pabich, T. F. Donahue, *Genes Dev.* **6**, 2463 (1992).
22. W. J. Feaver *et al.*, *Cell* **75**, 1379 (1993); J. Q. Svestrup *et al.*, *ibid.* **80**, 21 (1995).
23. D. A. Wassarman and J. A. Steitz, *Nature* **349**, 463 (1991).
24. J. Venema and D. Tollervy, *Yeast* **11**, 1629 (1995).
25. S. L. Gee and J. G. Conboy, *Gene* **140**, 171 (1994).
26. S. B. Bairn, D. F. Pietras, D. C. Eustice, F. Sherman, *Mol. Cell. Biol.* **5**, 1839 (1985).
27. Cellular Ded1p-PA protein was detected by indirect immunofluorescence microscopy [J. V. Kilmartin and A. E. Adams, *J. Cell Biol.* **98**, 922 (1984)]. Cells were grown to 1 OD<sub>600</sub> unit, collected by filtration, washed extensively in 0.1 M potassium phosphate (pH 6.5), and then fixed in 0.1 M potassium phosphate (pH 6.5) buffer containing 3.7% formaldehyde for 10 min. The formaldehyde-fixed cells were digested with zymolyase 100T (Seikagaku America, Rockville, MD) for 40 min at 37°C and washed three times in a phosphate-buffered saline (PBS) solution containing 1 M sorbitol. Cells were then treated with methanol (6 min) and acetone (30 s) at –20°C and resuspended in PBL [PBS, bovine serum albumin (1 mg/ml), and 100 mM lysine] to which purified normal rabbit IgG (3.5 mg/ml) was added at 1:50 dilution for staining overnight at room temperature. The next day, cells were washed three times in PBL, and the secondary antibody, Texas Red-conjugated goat antibody to rabbit IgG (Jackson Labs), was added at 1:50 dilution and incubated at room temperature for 90 min. Cells were then washed again in PBL and stained with 4',6-diamino-2-phenylindole (DAPI) (0.5 μg/ml). Cells were applied to slides with an equal volume of Citifluor (Marivac, Halifax, Nova Scotia, Canada) and

visualized with a Zeiss Axiophot microscope with Normarski optics. Texas Red and ultraviolet filters were used to detect Texas Red- and DAPI-stained images, respectively.

28. T.-H. Chang, unpublished data.
29. We thank K. Arndt, A. Hinnebusch, P. Linder, P. Sarnow, K. Struhl, and D. Wolgemuth for plasmids and strains; Y. Liu and A. Tartakoff for performing the in situ hybridization experiments; M. Leibowitz for

advice on yeast translation extracts; K. Arndt, T. Donahue, J. Hershey, A. Hinnebusch, K. Madura, W. Merrick, A. Sachs, N. Sonenberg, and J. Woolford for helpful discussions; and J. Abelson for support. Supported by funds from Ohio State University, NIH grant GM48752, and an American Cancer Society (Ohio Division) grant (T.-H.C.).

8 November 1996; accepted 27 January 1997

## Structure of a Protein Photocycle Intermediate by Millisecond Time-Resolved Crystallography

Ulrich K. Genick,\*† Gloria E. O. Borgstahl,\*†‡ Kingman Ng,†§ Zhong Ren,† Claude Pradervand, Patrick M. Burke,|| Vukica Srajer, Tsu-Yi Teng, Wilfried Schildkamp, Duncan E. McRee, Keith Moffat, Elizabeth D. Getzoff

The blue-light photoreceptor photoactive yellow protein (PYP) undergoes a self-contained light cycle. The atomic structure of the bleached signaling intermediate in the light cycle of PYP was determined by millisecond time-resolved, multiwavelength Laue crystallography and simultaneous optical spectroscopy. Light-induced trans-to-cis isomerization of the 4-hydroxycinnamyl chromophore and coupled protein rearrangements produce a new set of active-site hydrogen bonds. An arginine gateway opens, allowing solvent exposure and protonation of the chromophore's phenolic oxygen. Resulting changes in shape, hydrogen bonding, and electrostatic potential at the protein surface form a likely basis for signal transduction. The structural results suggest a general framework for the interpretation of protein photocycles.

Photoreceptors link light to life. Yet, understanding the molecular mechanisms for light-induced signal transduction has been limited by difficulties in obtaining and stabilizing light-activated conformations of suitable protein samples long enough for conventional structural studies by nuclear magnetic resonance or x-ray diffraction. Thus, three-dimensional structures known for photoactive proteins (1, 2) all describe proteins in their dark-state conformations. Here we present the structure of the light-activated, long-lived intermediate (*I*<sub>2</sub>) in the photocycle of PYP, as determined by time-resolved, multiwavelength Laue x-ray diffraction at a spatial resolution of 1.9 Å and a time resolution of 10 ms. This structure is expected to be

the biologically important signaling state.

PYP is the 125-residue, 14-kD cytosolic photoreceptor (3, 4) proposed to mediate negative phototaxis (5) in the phototrophic bacterium *Ectothiorhodospira halophila*. The photocycle kinetics in PYP crystals (6, 7) resemble those in solution (4, 8). After photon absorption (wavelength of maximum absorbance  $\lambda_{\text{max}} \sim 446$  nm), ground-state PYP (P) converts rapidly ( $\ll 10$  ns) to a red-shifted intermediate (*I*<sub>1</sub>), then quickly ( $k \approx 1 \times 10^4$  s<sup>-1</sup>) to a bleached, blue-shifted intermediate (*I*<sub>2</sub>). Spontaneous return of *I*<sub>2</sub> to P by a relatively slow process ( $k \approx 2$  to 3 s<sup>-1</sup>) completes the photocycle. One proton is taken up by PYP during formation of *I*<sub>2</sub> and released upon return to P (9). The 4-hydroxycinnamyl chromophore (Fig. 1A), covalently attached to Cys<sup>69</sup> through a thioester linkage, is proposed to photoisomerize during the photocycle (10, 11). In the ground- or dark-state structure of PYP determined at 1.4 Å resolution (2), the yellow, anionic chromophore (10, 12) forms a hydrogen bond with a buried glutamic acid within a hydrophobic core, protected from solvent.

The short lifetime of the *I*<sub>2</sub> intermediate and the need to simultaneously record optical data presented challenges beyond those encountered in previous Laue crystallographic studies (13). Specific features of our experimental system and techniques

U. K. Genick, G. E. O. Borgstahl, P. M. Burke, D. E. McRee, E. D. Getzoff, Department of Molecular Biology, Scripps Research Institute, 10550 North Torrey Pines Road, La Jolla, CA 92037, USA.

K. Ng, Z. Ren, C. Pradervand, V. Srajer, T.-Y. Teng, W. Schildkamp, K. Moffat, Department of Biochemistry and Molecular Biology, University of Chicago, 920 East 58th Street, Chicago, IL 60637, USA.

\*These authors contributed equally to this work.

†These authors made major contributions to time-resolved studies on photoactive yellow protein.

‡Present address: University of Toledo, Department of Chemistry, Toledo, OH 43606, USA.

§Present address: Eli Lilly and Company, Lilly Corporate Center, Indianapolis, IN 46285, USA.

||Present address: Department of Pathology, University of Utah School of Medicine, Salt Lake City, UT 84132, USA.